Available online at www.sciencedirect.com
ScienceDirect
Ceramics International 38 (2012) 635–640
CERAMICS INTERNATIONAL
www.elsevier.com/locate/ceramint

Synthesis and characterization of Fe^{3+} doped titanium dioxide nanopowders

Biljana Babić [a,*], Jelena Gulicovski [a], Zorana Dohčević-Mitrović [b], Dušan Bučevac [a], Marija Prekajski [a], Jelena Zagorac [a], Branko Matović [a]

[a] Institute of Nuclear Sciences "Vinca", University of Belgrade, P.O. Box 522, 11000 Belgrade, Serbia
[b] Institute of Physics, University of Belgrade, Pregrevica 118, P.O. Box 68, 11080 Belgrade, Serbia

Received 15 July 2011; received in revised form 22 July 2011; accepted 23 July 2011
Available online 30th July 2011

Abstract

Titanium dioxide nanopowders, doped with different amounts of Fe^{3+} ions (0.3–5 mass%), were synthesized by acid-catalyzed sol–gel method in a non-aqueous medium. The obtained powders were characterized by X-ray diffraction (XRD), scanning electron microscopy (SEM), Raman spectroscopy and determination of izoelectric points as well as particle diameters. Careful investigation of porous structure was provided by application of nitrogen adsorption–desorption method. Structure analysis showed that the obtained nanopowders exhibited the anatase crystal structure, independent of the amount of iron dopants. The presence of Fe^{3+} ions in anatase decreases the value of isoelectric point of undoped TiO_2. Unlike crystal structure, porosity parameters are strongly affected by the amount of iron ions incorporated in TiO_2 lattice. The mesoporosity of TiO_2 can be successfully controlled by changing the amount of iron dopants.

Keywords: A. Sol–gel process; D. TiO_2; Surface properties

1. Introduction

Titanium oxide nanoparticles are widely investigated due to their unique properties such as high stability, long lasting, mechanical, optical and electrochemical properties. The wide applications of TiO_2 nanoparticles as: anti-bacterial materials [1], UV-protectors [2], materials in environmental protection [3,4], photocatalyst [5–7], etc. demand general strategy for synthesis of TiO_2 in large quantities.

One of the most common methods is sol–gel processing in organic solvents under exclusion of water [5,8]. These processes involve the reaction of metal oxide precursor with organic solvent as a source of oxygen. These reactions take place at lower temperatures and allow mixing of species at molecular level. TiO_2 nanopowders, obtained by sol–gel method, usually have developed porosity, but shape and dimensions of pores are difficult to control [9,10].

The photocatalytic activity of TiO_2 depends on crystal structure, particle size, surface area, porosity, etc. A wide range of transitional metal ions, especially iron, were used as dopants for TiO_2 to improve its photocatalyst properties. Literature data show significant disagreements about the influence of doped iron on photocatalytic activity of TiO_2 [7,11–15]. The reason for that is twofold. The certain concentration of iron dopants near the surface of particle will strongly influence on charge transfer and on structure and porous properties of TiO_2, at the same time. Although the reports about synthesis of iron doped TiO_2 are numerous, the investigations of the influence of dopant metal ions on surface properties and porosity of TiO_2 nanoparticles are rare [16,17].

To our knowledge, only few paper, consider the isoelectric point of Fe^{3+} doped TiO_2 [18,19]. This characteristic is very important for the application of these materials in aqueous solutions.

The aim of this work is to estimate optimal synthesis conditions for obtaining samples of desired structure and surface properties of Fe^{3+} doped TiO_2 nanopowders which were synthesized by sol–gel method in non-aqueous medium. The influence of the amount of iron dopant on structure and surface properties of TiO_2 samples was investigated. Samples were characterized by X-ray and Raman spectroscopy and SEM analysis. In addition to the above mentioned methods,

* Corresponding author. Tel.: +381 11 3408224; fax: +381 11 3408224.
E-mail address: babicb@vinca.rs (B. Babić).

0272-8842/$36.00
doi:10.1016/j.ceramint.2011.07.053

determination of isoelectric point, as well as the particle size was performed in this study. Special attention was dedicated to investigation of the specific surface and porosity of obtained samples, determinated by BET method.

2. Experimental

2.1. Synthesis of doped TiO_2 samples

TiO_2 gels, doped with Fe^{3+}, were prepared by modified acid-catalyzed sol–gel method in a non-aqueous medium [5]. The sols were prepared by adding of 2 M solution of nitric acid to a solution of titanium isopropoxide $C_{12}H_{28}O_4Ti$ (97%, Aldrich) in anhydrous ethanol (99.5%, Superlab), at room temperature, under continuous stirring. The molecular ratios of Ti/ethanol/H_2O/nitric acid were 1/18/3/0.08. A corresponding amount of $Fe(NO_3)_3$ (p.a., Superlab) was dissolved in nitric acid solution before mixing with titanium isopropoxide. The amount of $Fe(NO_3)_3$ was adjusted so the final mass% of Fe^{3+} in TiO_2 powders was 0.3; 0.5; 1.0; 2.0; 3.0 and 5.0.

In each case, sols were stirred for 10 min, sealed and placed 5 days at room temperature. Formed gels were drying at 60 °C, for 24 h, on air. After drying samples were heated to obtain anatase crystallized phase and to remove traces of organic substances. Thermal treatment was carried out at 400 °C for 2 h, in air.

2.2. Characterization of doped TiO_2 samples

Adsorption and desorption isotherms of N_2 were measured on SBA-15 samples at −196 °C using the gravimetric McBain method. The specific surface area, S_{BET}, pore size distribution, mesopore including external surface area, S_{meso}, micropore volume, V_{mic}, for the samples were calculated from the isotherms. Pore size distribution was estimated by applying BJH method [19] to the desorption branch of isotherms and mesopore surface and micropore volume were estimated using the high resolution α_s plot method [20–22]. Micropore surface, S_{mic}, was calculated by subtracting S_{meso} from S_{BET}.

Field emission scanning electron microscopy (SEM) analysis was carried out on doped TiO_2 samples using a Hitachi 480 microscope.

Doped TiO_2 samples were characterized by recording their powder X-ray diffraction (XRD) patterns on a Siemens D500 X-ray diffractometer using Cu Kα radiation with a Ni filter. The 2θ angular regions between 5 and 80° were explored at a scan rate of 1°/s with the angular resolution of 0.02° for all XRD tests. Crystallite size was calculated using Scherrer equation.

Raman scattering measurements were performed at room temperature on micro-Raman system using Jobin-Yvon T64000 triple spectrometer. The Raman spectra were excited with the 514.5 nm of the Ar^+/Kr^+ laser operating at low incident power in order to avoid sample heating.

A Zetasizer Nano with 633 nm He–Ne laser equipped with an MPT Autotitrator manufactured by Malvern (Malvern, UK) was used to determine the isoelectric point of pure and Fe^{3+} doped titania samples by a potentiometric titration. This instrument measures particle sizes from 0.6 nm to 6 μm. A 0.05 g of titania samples were dispersed in 25 ml of 0.01 and 0.1 mol dm^{-3} KNO_3 and pH of suspensions were adjusted at pH ≈ 3. The samples were shaken mechanically and equilibrated in PVC vessels for 24 h at room temperature. Then, the samples were placed in a sample container and potentiometric titrations were performed with 0.01 mol dm^{-3} KOH from pH = 3 to pH = 9. Zeta, ζ, potentials were calculated by the instrument software (Smoluchowski equation). Agglomerated particle diameters were measured simultaneously with electrokinetic potential of the pure and Fe^{3+} doped titania single particle.

3. Results and discussion

According to X-ray diffraction analysis, the obtained powders are single phase, independent of dopant concentration in the range investigated (Fig. 1). Peaks related to isolated iron-bearing phases are not observed. All of solid solution powders exhibit the anatase (TiO_2) crystal structure, which is in agreement with literature data [13–15,17,23]. Fig. 1 also shows that peaks are very broad which indicates small crystallite size and/or strain. It was found that the crystallite size lies in the nanometric range (10–11 nm). Adan and et al. in their work claim that maximum solubility of iron cations inside anatase structure is close to 1.5 mass% [18]. According to results in this work all of 5 mass% of Fe^{3+} was successfully incorporated in anatase crystal lattice.

The Raman spectra of Fe^{3+} doped TiO_2 are presented in Fig. 2. Raman modes presented in Fig. 2 are characteristic for anatase phase with no traces of iron oxide phase indicating that the doped samples are solid solutions. The most prominent Raman E_g mode in the 0.3% Fe doped TiO_2 is shifted to higher frequencies regarding its bulk counterpart [24] and is positioned at 145 cm^{-1} (Fig. 3). The shift of this mode to

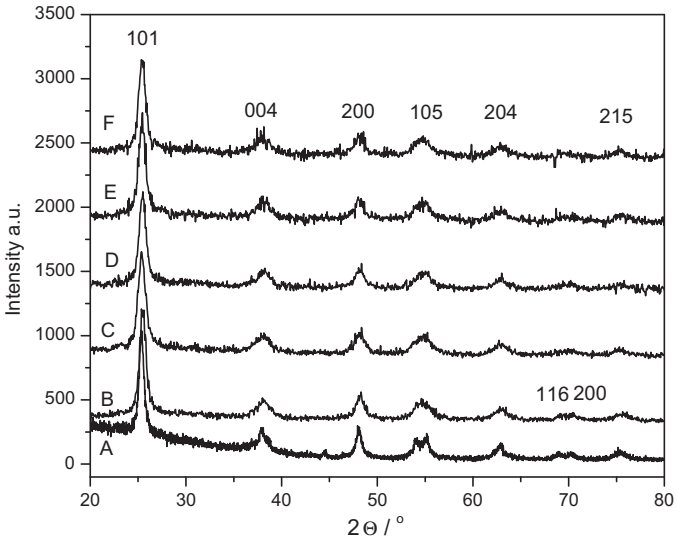

Fig. 1. X-ray diffraction patterns of Fe^{3+} doped TiO_2 samples (Fe^{3+} mass%: A-0, B-0.3, C-0.5, D-1, E-3, F-5).

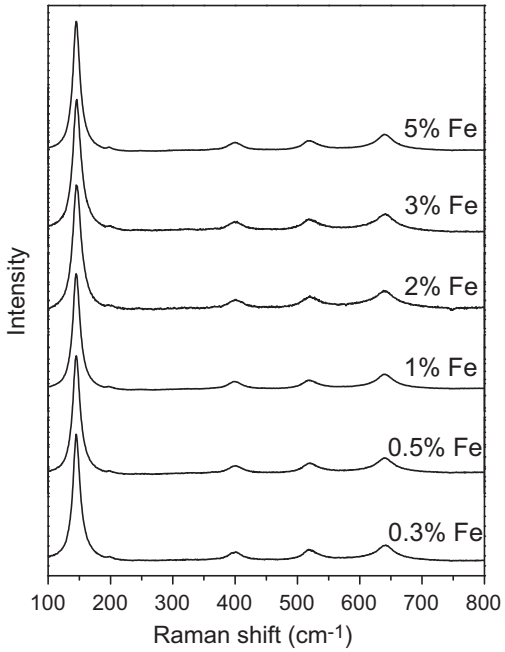

Fig. 2. Room temperature Raman spectra of Fe^{3+} doped TiO_2 samples.

higher frequencies and its asymmetry on the high energy side is characteristic for small crystallites.

With increasing of the Fe^{3+} up to the 3 mass% the E_g mode undergoes further shift to higher energies (see Fig. 2) indicating that Fe entered substitutionally into titania lattice. When the Fe content reaches 5 mass%, the E_g mode exhibits redshift to lower frequency. It is believed that such behavior originates from electron-molecular vibrational coupling due to the excess electrons present in titania lattice by increasing of Fe content [25]. Previous investigation also confirms that Fe based phases are not revealed by Raman spectra [26].

The zeta potential of pure and Fe^{3+} doped titania samples (0.3, 3 and 5 mass% of iron) in different concentrations of aqueous KNO_3 solutions at 25 °C was determined as a function

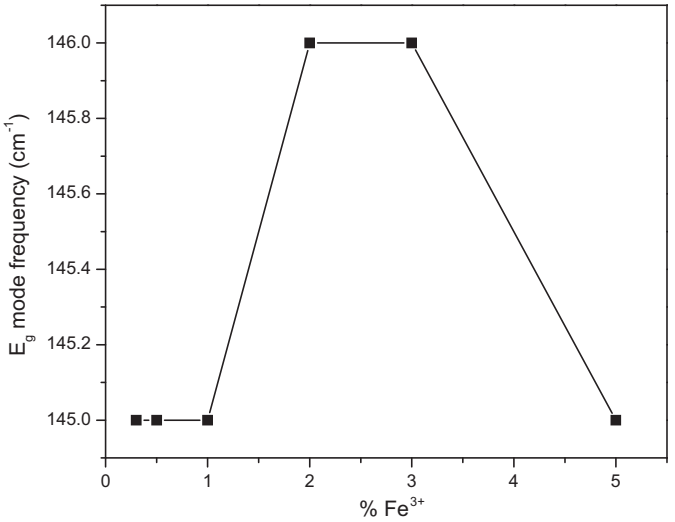

Fig. 3. Behavior of the E_g mode frequency with increasing Fe^{3+} content.

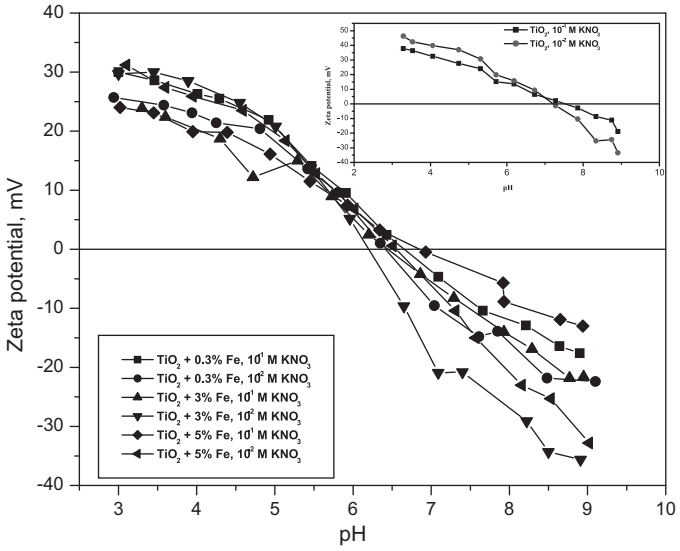

Fig. 4. The zeta potential of Fe^{3+} doped titania samples as a function of pH for different concentration of KNO_3. Inset: the zeta potential of pure TiO_2.

of pH, and the results are presented in Fig. 4. The titration started in acid region where titania surface is positively charged and value of zeta potential has a positive sign. The value of zeta potential decrease with increasing dispersion pH and position of the common intersection point appears to be at pH = 7.25 ± 0.2 and represents the isoelectric point of synthesized titania (Fig. 4, inset). Literature data show wide range of different values for isoelectric point of pure anatase which were summarized by Kosmulski [27,28]. Presence of Fe^{3+} ions in titania crystal lattice can cause shifts in isoelectric point due to changes in cation coordination, structural charge, ion exchange capacity, etc. These statements are confirmed by results of isoelectric points of Fe^{3+} doped titania samples which are presented in Fig. 4. The influence of doped iron ions on the zeta potential of the TiO_2 samples is notable. Obtained results

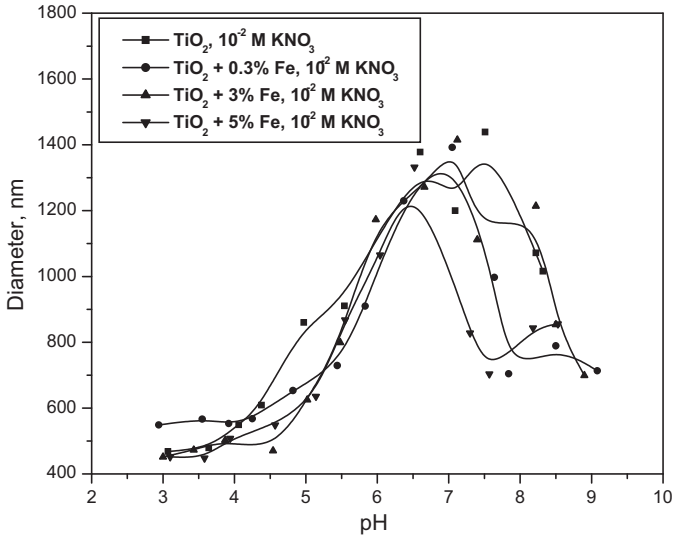

Fig. 5. The dependence of pure and Fe^{3+} doped titania particle diameters on suspension pH in KNO_3 solutions.

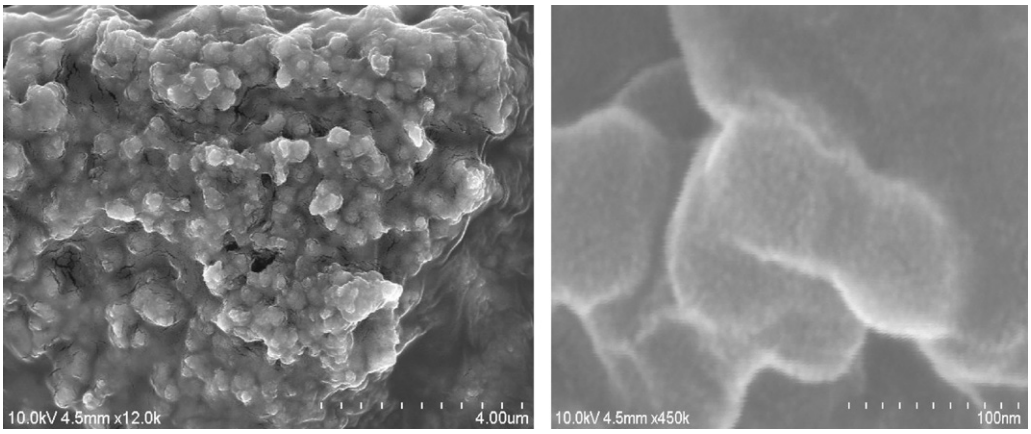

Fig. 6. SEM images of Fe^{3+} doped TiO_2 sample (Fe^{3+} mass% = 3).

show that the pH_{iep} decreases and appears to be at pH = 6.5 ± 0.2 for all samples which means that the amount of doped iron does not change the value of pH_{iep}. The trivalent Fe^{3+} ions are weak acids and their presence at titania lattice make overall surface more acidic.

Results obtained in this paper are in disagreement with results cited in Ref. [18]. The authors obtained that isoelectric point is function of the amount of iron incorporated in titania samples. This disagreement in the results of pH_{iep} in Ref. [18] and in this work may arise from different way of preparation of samples.

Fig. 5 presents the dependence of pure and doped titania particle diameter on dispersion pH in 0.01 M KNO_3 solution. The agglomeration is not a function of ionic strength of KNO_3 solution, in other words for the both concentrations of KNO_3 solutions (0.01 and 0.1 M) the diameter size increases with increasing pH of dispersion while the rapid increase i.e. agglomeration is note at pH values which are close to the value of isoelectric point of samples. This behavior can be ascribed to the lowering of the thickness of the diffuse part of the electrical double layer around pure and doped titania particles and stronger interaction between NO_3^- ions and the pure and doped titania particle particles in more concentrated solutions. For all samples particle diameter is similar, independent of the amount of doped iron in titania. This also confirms that Fe^{3+} ions are incorporated in crystal lattice of anatase.

SEM images of Fe^{3+} doped TiO_2 sample (Fe^{3+} mass% = 3) is given in Fig. 6. The morphology of the obtained powder shows that particles have the large distribution of shape and dimensions. It is worth noting that grains consist of agglomerates of small particles.

Nitrogen adsorption isotherms, as the amount of N_2 adsorbed as function of relative pressure at −196 °C, are shown in Fig. 7. According to the IUPAC classification [29] isotherms are of type-IV and with a well defined hysteresis loops which are associated with mesoporous materials. Specific surface areas calculated by BET equation, S_{BET}, are listed in Table 1. Porous parameters of pure TiO_2, synthesized by the same procedure, are also presented in Table 1, for comparison. It can be seen that incorporation of small amounts of iron in the lattice of TiO_2 decreases S_{BET}. However, higher amounts of iron dopant significantly increase the overall specific surface.

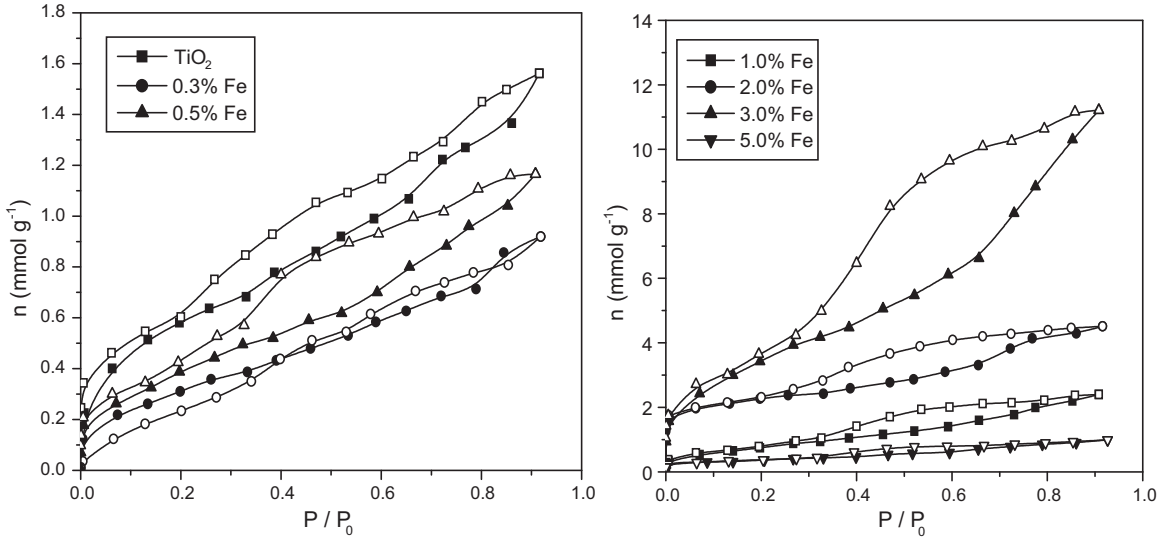

Fig. 7. Nitrogen adsorption isotherms of pure and Fe^{3+} doped TiO_2 samples: (a) pure TiO_2, 0.3 and 0.5 mass% of Fe^{3+}; (b) 1.0, 2.0, 3.0 and 5.0 mass% of Fe^{3+}. Solid symbols – adsorption, open symbols – desorption.

Table 1
Porous properties of Fe-doped TiO_2 samples.

Sample	S_{BET} ($m^2\ g^{-1}$)	S_{meso} ($m^2\ g^{-1}$)	S_{mic} ($m^2\ g^{-1}$)	S_{meso}/S_{mic}	V_{mic} ($m^3\ g^{-1}$)
TiO_2	29	14	15	1.3	0.016
0.3% Fe	47	21	26	0.8	0.026
0.5% Fe	26	16	10	1.6	0.011
1.0% Fe	32	18	14	1.3	0.012
2.0% Fe	62	38	24	1.6	0.033
3.0% Fe	178	39	139	0.3	0.104
5.0% Fe	278	200	78	2.6	0.123

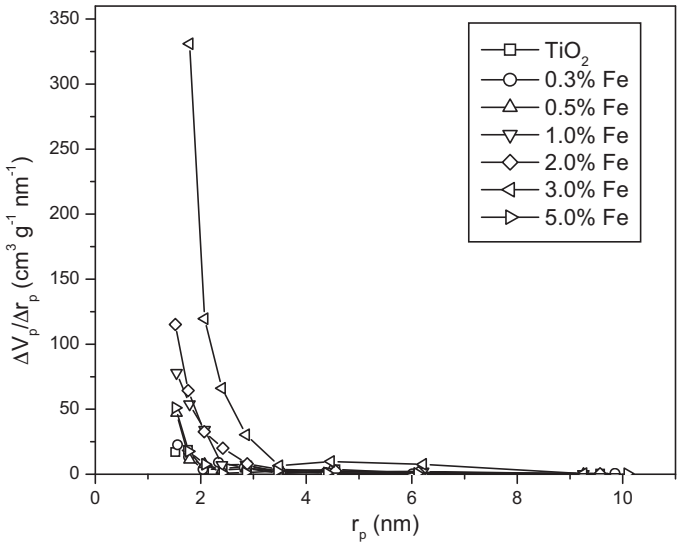

Fig. 8. Pore size distribution (PSD) of pure and Fe^{3+} doped TiO_2 samples.

Pore size distribution (PSD) of Fe^{3+} doped TiO_2 samples is given in Fig. 8. The distribution is continual and shows that pore radius, in all samples, is below 4 nm, but in the mesoporous region. Also, the amount of mesopores with larger radius increase with increasing the quantity of iron dopant.

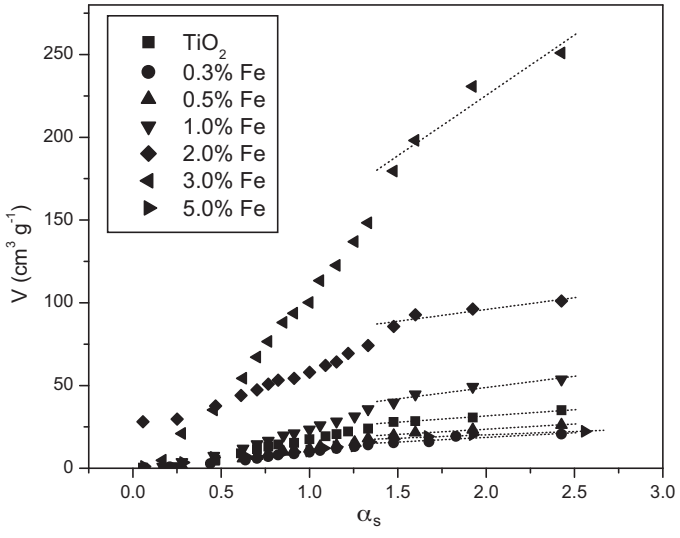

Fig. 9. α_s-Plots for nitrogen adsorption isotherms of pure and Fe^{3+} doped TiO_2 samples.

α_s plots, obtained on the basis of the standard nitrogen adsorption isotherm are shown in Fig. 9. The straight line in the medium α_s region gives a mesoporous surface area including the contribution of external surface, S_{meso}, determined by its slope, and micropore volume, V_{mic}, is given by the intercept. Calculated porosity parameters (S_{meso}, S_{mic}, V_{mic}) are given in Table 1. For the samples with different amount of iron dopant, porosity parameters are function of percentage of iron ions incorporated in TiO_2 lattice and ratio S_{meso}/S_{mic} varies. Mesoporous surface slightly decrease with increasing the amount of doped iron up to 3 mass%. Sample with 5 mass% has significantly larger mesoporous surface comparing with the other samples. As discussed above, the mesoporosity of TiO_2 can be successfully controlled by changing the amount of iron dopant.

By inspection of data from Table 1 one can see that pure TiO_2 and sample of TiO_2 with 2 mass% have similar porous properties. For samples with concentration of iron ions below 2 mass%, the smaller ionic radius of iron ions, in comparison with ionic radius of titanium, reduces the size of the crystal lattice. Also, at lower doped quantities, the concentration of iron ions is very small and their influence is localized. As a consequence, particles are smaller, micropores on surface of particle are smaller and mesopores between two particles are smaller, too. At higher concentrations of iron ions (above 2 mass%) the influence of single Fe ions is overlapped, since they are close to each other. As a result, the shapes of particles are irregular and the space between particles is larger, i.e. microporous and mesoporous surfaces are larger. To our knowledge, systematic investigations which can approve prediction of porous properties of final samples as a function of synthesis conditions were not provided, until now.

4. Conclusions

Fe^{3+} doped titanium dioxide nanopowders were successfully synthesized by acid-catalyzed sol–gel method in non-aqueous medium. Characterization of obtained nanopowders has shown that all samples have anatase structure and Fe^{3+} ions are completely incorporated in TiO_2 lattice. The secondary crystalline phases containing Fe was not detected, even in samples with 5 mass% of iron. The presence of Fe^{3+} ions in anatase decreases the value of isoelectric point of undoped TiO_2. Obtained results show that the pH_{iep} decreases and appears to be at $pH = 6.5 \pm 0.2$ for all doped samples which means that the amount of doped iron does not change the value of pH_{iep}. The amount of doped iron strongly influences on

porous properties of obtained material. By the choice of appropriated amount of iron in starting solutions it is possible to control the ratio between mesoporous and microporous surface.

Acknowledgement

This project was financially supported by the Ministry of Science and Technology of the Republic of Serbia (Project number: 45012).

References

[1] R. Dastjerdi, M. Montazer, A review on the application of inorganic nano-structured materials in the modification of textiles: focus on anti-microbial properties, Colloids Surf. B 79 (2010) 5–18.
[2] K. Han, M. Yu, Study of the preparation and properties of UV-blocking fabrics of a PET/TiO_2 nanocomposite prepared by in situ polycondensation, J. Appl. Polym. Sci. 100 (2006) 1588–1593.
[3] D. Li, H. Haneda, S. Hishita, N. Onashi, Visible-light-driven N-F-codoped TiO_2 photocatalysts. 2. Optical characterization, photocatalysis, and potential application to air purification, Chem. Mater. 17 (2005) 2596–2602.
[4] L. Cermenati, P. Pichat, C. Guillard, A. Albini, Probing the TiO_2 photocatalytic mechanisms in water purification by use of quinoline, photo-fenton generated $OH^{\bullet}$ radicals and superoxide dismutase, J. Phys. Chem. B 101 (1997) 2650–2658.
[5] S. Boujday, F. Wunsch, P. Portes, J.F. Bocquet, C. Colbeau-Justin, Photocatalytic and electronic properties of TiO_2 powders elaborated by sol–gel route and supercritical drying, Sol. Energy Mater. Sol. Cells 83 (2004) 421–433.
[6] C. Lee, R.H. Lin, C.Y. Yang, M.H. Lin, W.Y. Wang, Preparations and characterization of novel photocatalysts with mesoporous titanium dioxide (TiO_2) via a sol–gel method, Mater. Chem. Phys. 109 (2008) 275–280.
[7] M. Ni, M.K.H. Leung, D.Y.C. Leung, K. Sumathy, A review and recent developments in photocatalytic water-splitting using TiO_2 for hydrogen production, Renew. Sustain. Energy Rev. 11 (2007) 401–425.
[8] C. Sung, K.Z. Fung, I.M. Hung, M.H. Hon, Synthesis of highly ordered and worm-like mesoporous TiO_2 assisted by tri-block copolymer, Solid State Ionics 179 (2008) 1300–1304.
[9] Q. Dai, Z. Zhang, N. He, P. Li, C. Yuan, Preparation and characterization of mesostructured titanium dioxide and its application as a photocatalyst for the wastewater treatment, Mater. Sci. Eng. C 8–9 (1999) 417–423.
[10] B. Xin, Z. Ren, P. Wang, J. Liu, L. Jing, H. Fu, Study on the mechanisms of photoinduced carriers separation and recombination for Fe^{3+}–TiO_2 photocatalysts, Appl. Surf. Sci. 253 (2007) 4390–4395.
[11] S. Liu, Y. Chen, Enhanced photocatalytic activity of TiO_2 powders doped by Fe unevenly, Catal. Commun. 10 (2009) 894–899.
[12] M.C. Wang, H.J. Lin, T.S. Yang, Characteristics and optical properties of iron ion (Fe^{3+})-doped titanium oxide thin films prepared by a sol–gel spin coating, J. Alloys Compd. 473 (2009) 394–400.
[13] C.A. Castro-Lopez, A. Centeno, S.A. Giraldo, Fe-modified TiO_2 photocatalysts for the oxidative degradation of recalcitrant water contaminants, Catal. Today 157 (2010) 119–124.
[14] Z. Li, W. Shen, W. He, X. Zu, Effect of Fe-doped TiO_2 nanoparticle derived from modified hydrothermal process on the photocatalytic degradation performance on methylene blue, J. Hazard. Mater. 155 (2008) 590–594.
[15] Y. Wang, Z.H. Jiang, F.J. Yang, Effect of Fe-doping on the pore structure of mesoporous titania, Mater. Sci. Eng. B 134 (2006) 76–79.
[16] M. Zhou, J. Yu, B. Cheng, H. Yu, Preparation and photocatalytic activity of Fe-doped mesoporous titanium dioxide nanocrystalline photocatalysts, Mater. Chem. Phys. 93 (2005) 159–163.
[17] K. Wantala, D. Tipayarom, L. Laokiat, N. Grisdanurak, Sonophotocatalytic activity of methyl orange over Fe(III)/TiO_2, React. Kinet. Catal. Lett. 97 (2009) 249–254.
[18] C. Adan, J. Carbajo, A. Bahamonde, A. Martinez-Arias, Phenol photodegradation with oxygen and hydrogen peroxide over TiO_2 and Fe-doped TiO_2, Catal. Today 143 (2009) 247–252.
[19] E.P. Barret, L.G. Joyner, P.P. Halenda, The determination of pore volume and area distributions in porous substances. I. Computations from nitrogen isotherms, J. Am. Chem. Soc. 73 (1951) 373–380.
[20] K. Kaneko, C. Ishii, M. Ruike, H. Kuwabara, Origin of superhigh surface area and microcrystalline graphitic structures of activated carbons, Carbon 30 (1992) 1075–1088.
[21] M. Kruk, M. Jaroniec, K.P. Gadakaree, Nitrogen adsorption studies of novel synthetic active carbons, J. Colloid Interface Sci. 192 (1997) 250–256.
[22] K. Kaneko, C. Ishii, H. Kanoh, Y. Hanzawa, N. Setoyama, T. Suzuki, Characterization of porous carbons with high resolution α_s-analysis and low temperature magnetic susceptibility, Adv. Colloid Interface 76–77 (1998) 295–320.
[23] J.A. Navio, G. Colon, M. Macias, C. Real, M.I. Litter, Iron-doped titania semiconductor powders prepared by a sol–gel method. Part I: synthesis and characterization, Appl. Catal., A 177 (1999) 111–120.
[24] T. Ohsaka, F. Izumi, Y. Fujiki, Raman spectrum of anatase, TiO_2, J. Raman Spectrosc. 7 (1978) 321–324.
[25] Z.D. Dohčević-Mitrović, N. Paunović, M. Radović, Z.V. Popović, B. Matović, B. Cekić, V. Ivanovski, Valence state dependent room-temperature ferromagnetism in Fe-doped ceria nanocrystals, Appl. Phys. Lett. 96 (2010) 203104–203107.
[26] D. Bersani, P.P. Lottici, A. Montetnero, A micro-Raman study of iron-titanium oxides obtained by sol–gel synthesis, J. Mater. Sci. 35 (2000) 1–5.
[27] M. Kosmulski, pH-dependent surface charging and points of zero charge: III. Update, J. Colloid Interface Sci. 298 (2006) 730–741.
[28] M. Kosmulski, The pH-dependent surface charging and points of zero charge: V. Update, J. Colloid Interface Sci. 353 (2011) 1–15.
[29] K.S.W. Sing, D.H. Everett, R.A.W. Haul, L. Moscou, R.A. Pierotti, J. Rouquerol, et al., Reporting physisorption data for gas/solid systems with special reference to the determination of surface area and porosity, Pure Appl. Chem. 57 (1985) 603–619.